Electronic Supplementary Material (ESI) for Chemical Science.

Supporting Information

Americium preferred: Lanmodulin, a natural lanthanide-binding protein favors an actinide over lanthanides

Helena Singer †, Björn Drobot †, Cathleen Zeymer, Robin Steudtner* and Lena J. Daumann*

Table of Contents

1. Experimental Procedures

1.1. Molecular cloning, expression and protein purification of LanM

A synthetic gene coding for LanM from *M. extorquens* without its N-terminal signal sequence (amino acids 1-21) was ordered from TWIST Bioscience (USA) and subcloned into a modified pET29b expression vector coding for a C-terminal Strep-tag. This tag was used to avoid possible metal binding, as it would be the case for a His-tag. The amino acid sequence, molecular weight MW, and extinction coefficient ε_{280} of the construct are listed below:

MPTTTTKVDIAAFDPDKDGTIDLKEALAAGSAAFDKLDPDKDGTLDAKELKGRVSEADLKKLDPDNDGTLDKKEYLAAVEAQFKAANPD
NDGTIDARELASPAGSALVNLIRGSAWSHPQFEK

MW = 13.1 kDa, ε_{280} = 6990 M^{-1} cm^{-1}

The protein was produced in *E. coli* BL21 Gold in an overnight expression at 18 °C after induction with 0.5 mM IPTG. Cells were harvested by centrifugation and lysed by sonication in a lysis buffer containing 1.0 mg/ml lysozyme. Cleared cell lysate was loaded on a Strep-Tactin® affinity column (IBA, Germany). Protein purification was performed in the presence of EDTA following the standard protocol of the supplier: wash buffer (40 mM HEPES pH 8.0, 150 mM NaCl, 1 mM EDTA), elution buffer (40 mM HEPES pH 8.0, 150 mM NaCl, 1 mM EDTA, 2.5 mM d-desthiobiotin). The elution fraction was dialyzed twice against sample buffer (10 mM Tris/HCl pH 6.8, 100 mM KCl). The protein was concentrated in an Amicon® centrifugal device to a final concentration of 181 µM and subsequently aliquoted and flash-frozen in liquid nitrogen. The purity was confirmed by SDS-PAGE (figure S4).

To study the ability of the purified apo-LanM to bind Lns, metal titrations with different Lns at various pHs were performed using CD spectroscopy (figure S6, with Eu^{3+} at pH 6.7) and an Arsenazo III dye coupled assay (data not shown). Similar results were obtained as described by Cotruvo and coworkers,[1] confirming that the slightly modified LanM is also able to bind Lns with a high affinity.

1.2. Preparation of An and Ln working solutions

1.2.1. Actinide solutions

The used actinides and their decay products pose serious health hazards and should thus only be handled at institutions designed for their safe handling.

^{237}Np

5.0 mg $NpCl_4(dme)_2$ (dme = 1,2-dimethoxyethane) was dissolved in 1 mL tetrahydrofuran. The solution was added to an excess (i.e. 10 mg) of potassium graphite (KC_8) and stirred for 30 minutes showing a color change from pink to yellow-green. The potassium graphite was separated from the solution by centrifugation and the supernatant was evaporated until dryness. The residue was dissolved in 1 mL dimethyl sulfoxide (DMSO) yielding a greenish solution. This stock solution (c ≈ 9mM) was hence diluted (first: 1:100 v/v, second 1:3 v/v) to yield a solution of c ≈ 30µM Np^{3+} in DMSO.

^{242}Pu (92%) / ^{238}Pu (8%)

A 6 mM Pu(IV) stock solution (without Am) in 0.1 M HCl was used to produce a Pu^{3+} by electrochemical reduction. The potential was set to –0.6 V for Pu^{3+} production. After approximately 120 minutes, all Pu(IV) was reduced to Pu^{3+}. The pure Pu^{3+} solution was obtained as a result. The vial with the solution was wrapped with parafilm and stored inside an inert gas glovebox for one week before commencing with the preparation of a Pu^{3+} stock solution at pH 4. 2.75 mL of this solution was diluted with 6.75 mL of MilliQ water to a total volume of 9.5 mL. The initial concentration of the Pu^{3+} stock solution for titration to a pH of approximately 4 was therefore 3.6 mM. The final pH adjustment to pH 3.95 take place by the addition of aliquots of NaOH under a constant voltage of -0.4 V to prevent the formation of Pu(IV) polymers or colloids during the NaOH addition process. The final concentration of the Pu^{3+} solution was analyzed with liquid scintillation counting (LSC) and determined to be 3.4 mM.

^{243}Am (100%)

Am^{3+} stock solution (26 µM) in 0.001 M HCl was used.

^{248}Cm (97.3%) / ^{246}Cm (2.6%) / ^{245}Cm (0.04%) / ^{247}Cm (0.02%) / ^{244}Cm (0.009%)

A 7.3 mM stock solution of the long-lived curium isotopes in 1.0 M $HClO_4$ was used. In a first step, the background electrolyte was converted from $HClO_4$ to HCl. To 500 µl of the perchlorate solution were added 1.5 ml 5 M NaOH to shift the pH clearly in the alkaline region. Afterwards the solution was centrifuged (10 min with 13000 rpm) and the supernatant was discarded. The solid was dissolved in 500 µL 1 M HCl and the conversion repeated four times. The final concentration of the Cm^{3+} solution in 1 M HCl was analyzed with LSC and determined to be 7 mM.

1.2.2. Lanthanide solutions

All lanthanides Ln^{3+} were available as $LnCl_3$ hydrates. 10 mM stocks were prepared in MilliQ water and stored at – 20 °C until they were used.

1.3. Binding studies with TRLFS

Important: When working with actinides, special safety precautions need to be considered. All measurements were carried out in a radioactive controlled environment in compliance with regulations.

To study the binding of different lanthanides and/or actinides, fluorescence properties of Eu^{3+} and Cm^{3+} were used. All measurements were performed in a 2 mL quartz glass cuvette, and temperature was adjusted to 25 °C in the temperature-controlled cuvette holder. For sufficient and fast mixing, stirring speed of 1200 rpm was set. An excitation wavelength of 394 nm was chosen for binding studies regarding Eu^{3+}, for Cm^{3+} a wavelength of 396 nm was applied (Ekspla, NT230, ~5 ns pulse). The cuvette holder was connected to the spectrograph (Andor, SR-303i-A) via a light guide. Spectra were recorded with an ICCD (Andor iStar, DH320T-18U-63). Data deconvolution was performed with parallel factor analysis (PARAFAC, N-way toolbox for Matlab)[2] and is summarized in Figure S1.

All experiments were performed in a TRIS-KCl buffer (10 mM TRIS, 100 mM KCl, pH 6.7). This pH was chosen to mimic physiological conditions. With higher pH, most probably the amount of available Ln aquo ions might decrease due to hydrolysis. Ln solutions were available in 10 mM stocks in MilliQ water and were diluted to 1 mM in the buffer if required. Available An stock solutions (in detail described above) were adjusted to 30 µM with the buffer. For Cm^{3+} binding studies, a 5 µM solution of LanM in buffer was prepared while for studies with Eu^{3+} the frozen stocks with concentration of 181 µM were used. When working with Ans, a final concentration of 100 nM of Cm^{3+} was not exceeded which was found to be good compromise between sensitivity and radioactivity. For fluorescence studies with Eu^{3+}, an amount of 5.5 µM was used during the measurements.

Different experiments were carried out to shed light on various issues and will be described in the following. For competitive binding studies, different combinations of Ln and An were chosen.
Ln series: La^{3+}/Eu^{3+}, Ce^{3+}/Eu^{3+}, Pr^{3+}/Eu^{3+}, Nd^{3+}/Eu^{3+}, Sm^{3+}/Eu^{3+}, Gd^{3+}/Eu^{3+}, Tb^{3+}/Eu^{3+}, Dy^{3+}/Eu^{3+}, Ho^{3+}/Eu^{3+}, Er^{3+}/Eu^{3+}, Tm^{3+}/Eu^{3+}, Yb^{3+}/Eu^{3+}, Lu^{3+}/Eu^{3+}
An series: Np/Cm^{3+}, Pu/Cm^{3+}, Am^{3+}/Cm^{3+}, Nd^{3+}/Cm^{3+}

1.3.1. Eu^{3+}/Cm^{3+} titration to LanM

To see if the purified LanM is able to bind Eu^{3+} or Cm^{3+}, initial binding studies were performed to determine the exact amount of Eu^{3+} or Cm^{3+} which could be bound by LanM.

The protein LanM was diluted to a concentration of 1 µM in the buffer in a total volume of 1000 µL. A 1 mM Eu^{3+} solution was added in 0.5 and 1 µL steps until a concentration of 10 µM was reached. TRLFS parameters for the measurement were exponential step size 5+1*x, initial delay 288 µs, gate width 500 µs, accumulations 200, kinetic series length 5, gain 4000, 100 µm slit width, grating 300 l/mm.

A 5 µM dilution of LanM in buffer was titrated in 0.6 µL steps to 1000 µL of a 100 nM solution of Cm^{3+} in buffer. In total, 20 titration steps were performed to reach a concentration of 57 nM LanM. TRLFS parameters for the measurement were linear increasing step size 3+1*x, initial delay 275 µs, gate width 100 µs, accumulations 200, kinetic series length 25, gain 4000, 600 µm slit width, grating 600 l/mm.

1.3.2. A to Eu^{3+}-LanM or Cm^{3+}-LanM – Ln/An addition

In addition, it was tested if different subsequently added Lns or Ans have an impact on LanM which has prior bound to Eu^{3+} (Ln series) or Cm^{3+} (An series).

For experiments regarding the Ln series, 1 µM LanM was incubated with 5.5 µM Eu^{3+} for 10 minutes at room temperature with constant stirring. Then, 5.5 µM of Ln was added and immediately after the addition the data acquisition was started. The measurements were initially carried out in short intervals, with ongoing time the intervals were increased. Spectra were collected until no more changes occurred. TRLFS parameters for the measurement were exponential step size $5*e^{1x}$, initial delay 288 µs, gate width 200 µs, accumulations 200, kinetic series length 5, gain 400, 100 µm slit width, grating 300 l/mm.

The procedure for the An series was carried out in the same way but different concentration of An or Nd^{3+} and protein was used. 100 nM Cm^{3+} and the additional An or Nd was mixed in buffer. Shortly after addition of 18 nM LanM, the spectra collection was started. TRLFS parameters for the measurement were exponential step size $20*e^{0.27x}$, initial delay 275 µs, gate width 600 µs, accumulations 200, kinetic series length 5, gain 4000, 600 µm slit width, grating 1200 l/mm.

1.3.3. A/Eu^{3+} to LanM or A/Cm^{3+} to LanM – Ln/An competition

Focusing the differences of preferred Ln binding of LanM, 5.5. µM of Eu^{3+} and 5.5 µM of Ln (see Ln series) were added to the cuvette in buffer. Then 1 µM of LanM was added, and the mix was incubated for 24 hours at room temperature. Spectra were collected with parameters of linear increasing step size 3+3*x, initial delay 288 µs, gate width 500 µS, accumulations 200, kinetic series length 25,

gain 4000, input slit 100 µM, grating 300l/mm. Spectra were collected before addition of LanM, shortly after addition of the protein, and after 24 hours incubation period.

For experiments regarding the An series or Ln/An series, 100 nM of Cm^{3+} and 100 nM of Ans or Nd^{3+} (see An series) in the cuvette with buffer. Subsequently, 18 nM of LanM were added and it was incubated for 24 hours at room temperature. TRLFS parameters for the measurement were linear increasing step size 3+1*x, initial delay 275 µs, gate width 600 µs, accumulations 200, kinetic series length 25, gain 400, 600 µm slit width, grating 1200 l/mm. Spectra were collected before addition of LanM, shortly after addition of the protein, and after 24 hours incubation period.

1.4. Binding studies with CD spectroscopy

CD spectra were collected using a JASCO J-810 CD and ORD spectropolarimeter with thermostat-controlled cell holder in combination with software Spectra Manager Version 2.06.00.

Experiments to study a possible conformational change of apo-LanM and Eu^{3+}were carried out with frozen LanM stocks without further purification or washing procedure in a macro cuvette (QS) with 1 mm pathlength at 25 °C. For the stoichiometric titration with Eu^{3+}, 20 µM of apo-LanM were diluted in TRIS-KCl buffer (10 mM TRIS, 100 mM KCl, pH 6.7) to a final volume of 200 µL. The Eu^{3+} stock solution (10 mM) was prepared as described in 1.2.2. Each equivalent of metal corresponded to a volume of 0.4 µL of the Eu^{3+} stock. Collection of spectra was started 2 minutes after metal addition. Spectra were scanned from 180 – 300 nm with 1 nm bandwidth, 0.5 nm data pitch, 50 nm/min scan rate, D.I.T. 4 seconds. Three accumulations were acquired, and spectra were baseline corrected with a previously collected buffer sample. Due to small volume changes, no correction of concentration was applied.

2. Data analysis

2.1 Parallel factor analysis (PARAFAC)

Data from time resolved laser-induced fluorescence spectroscopy were analyzed using PARAFAC as implemented for Matlab R2020b as N-way toolbox for Matlab.[2] This approach was previously successful applied on the interaction of a protein (calmodulin) with Eu^{3+}.[3]

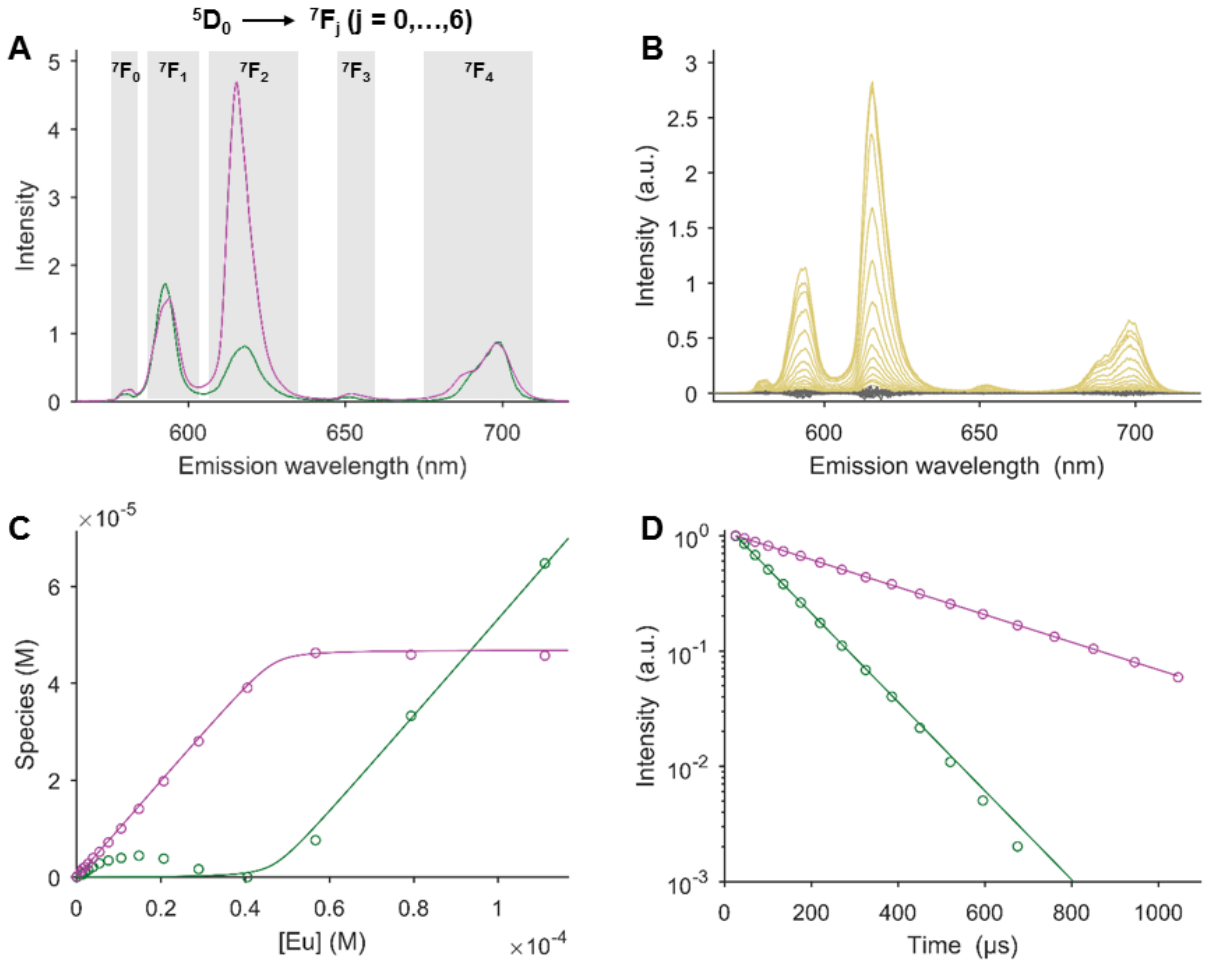

Figure S1. A The emission spectrum of Eu^{3+} consists of several electronic transitions. Its main transitions origin from the $^5D_0$ level to the J levels of the ground term ^7F with j = 0,…,6. Often transitions to the $^7F_5$ and $^7F_6$ transitions are not observable. Therefore, the graph shows only transitions up to j = 4. The ^7F_j level can split into a set of crystal field levels. The maximum number of crystal field induced split levels is given by 2j+1 and depends on the symmetry of the crystal field. This splitting is responsible for the unsymmetrical shape of individual $^5D_0 \rightarrow {}^7F_j$ transitions. The species assignment is supported by the emission spectra based on the PARAFAC calculation. The F_1/F_2 ratio of green spectrum is characteristic for the Eu^{3+} aquo ion. Changes in this ratio are indicative for Eu^{3+} complexation, here the formation of a Eu^{3+}-LanM complex. **B** Comparison of t_0 raw spectra (yellow) with the corresponding residuals demonstrate the goodness (grey) of the used PARAFAC model. **C** The distribution of the two PARAFAC species show the transition from the initial the Eu^{3+}-LanM complex (magenta) to the Eu^{3+} aquo ion (green) with increasing Eu^{3+} concentrations. **D** This assignment is further ensured by the luminescence lifetimes (τ_{aquo} = 113 ± 2 µs, $\tau_{Eu(III)\text{-}LanM}$ = 364 ± 3 µs). The extended lifetimes of Eu^{3+} complexes are usually explained by water molecule displacement from the Eu^{3+} coordination sphere.

2.2 Exchange kinetics

All exchange kinetics were fitted to an exponential decay including an offset term

$$I(t) = e^{-\frac{t}{\tau}} + c$$

Here t is the time, τ = 1/k the time constant and c the constant value corresponds to $I_{(t\rightarrow\infty)}$. Without exact knowledge about process details involved in the exchange of one f-element with another, the time constant is given as apparent time constant**.**

2.3 Monte Carlo approach for estimation of parameter errors

In order to provide robust estimates of parameter errors an Monto Carlo (MC) approach was used as previously described.[3] Synthetic generated noise of the same magnitude as the residuals was added to the data and the fitting procedure was repeated (1000 times). The synthetic data and corresponding fits for the kinetic experiments are given in Figure S2 and S3. All fitted constants c and time constants τ of the 1000 MC runs were used for the box plots in the main manuscript.

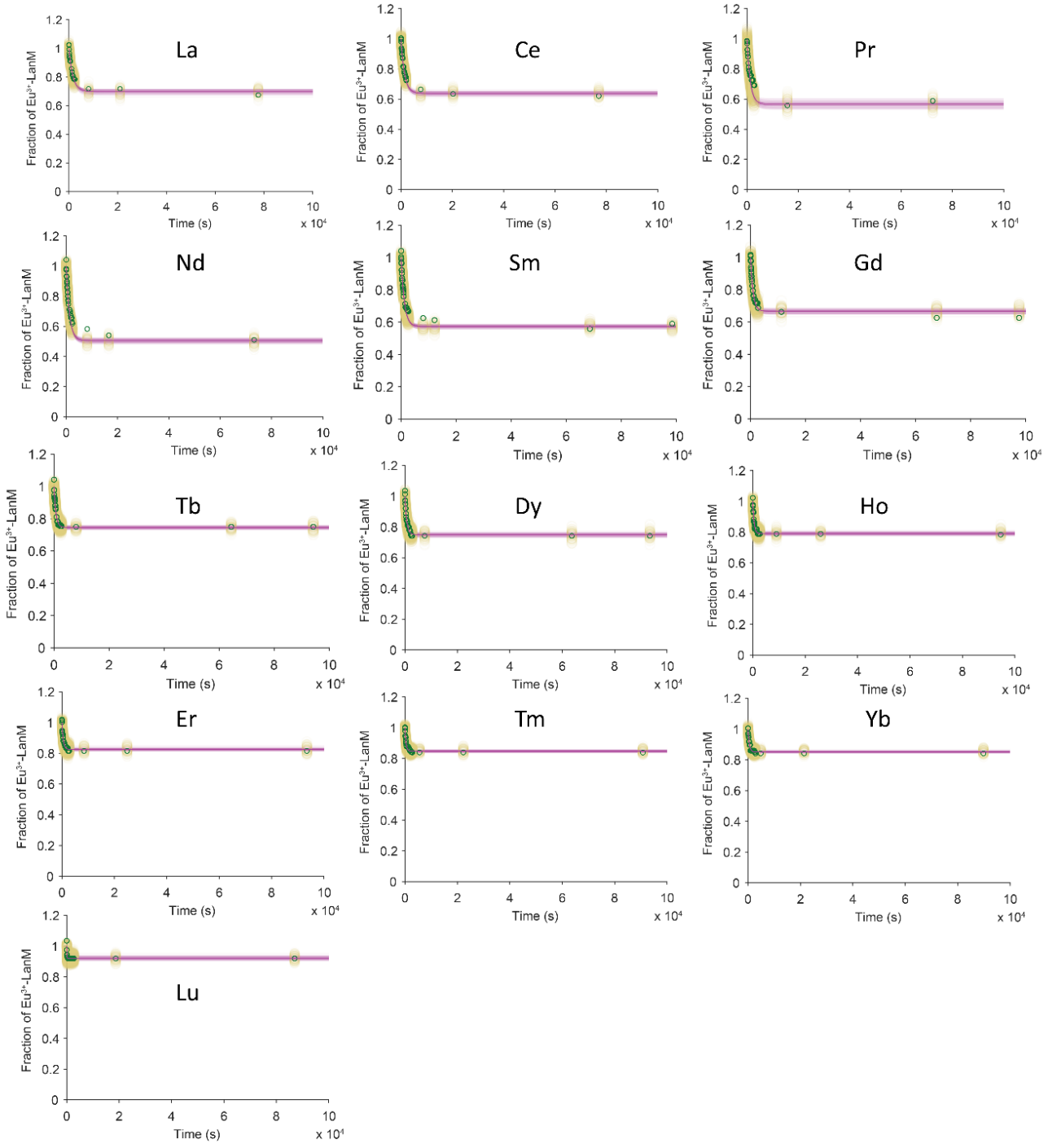

Figure S2. B MC approach for the exchange experiments with Eu^{3+}. MC in yellow compared to raw data in green (fits in magenta).

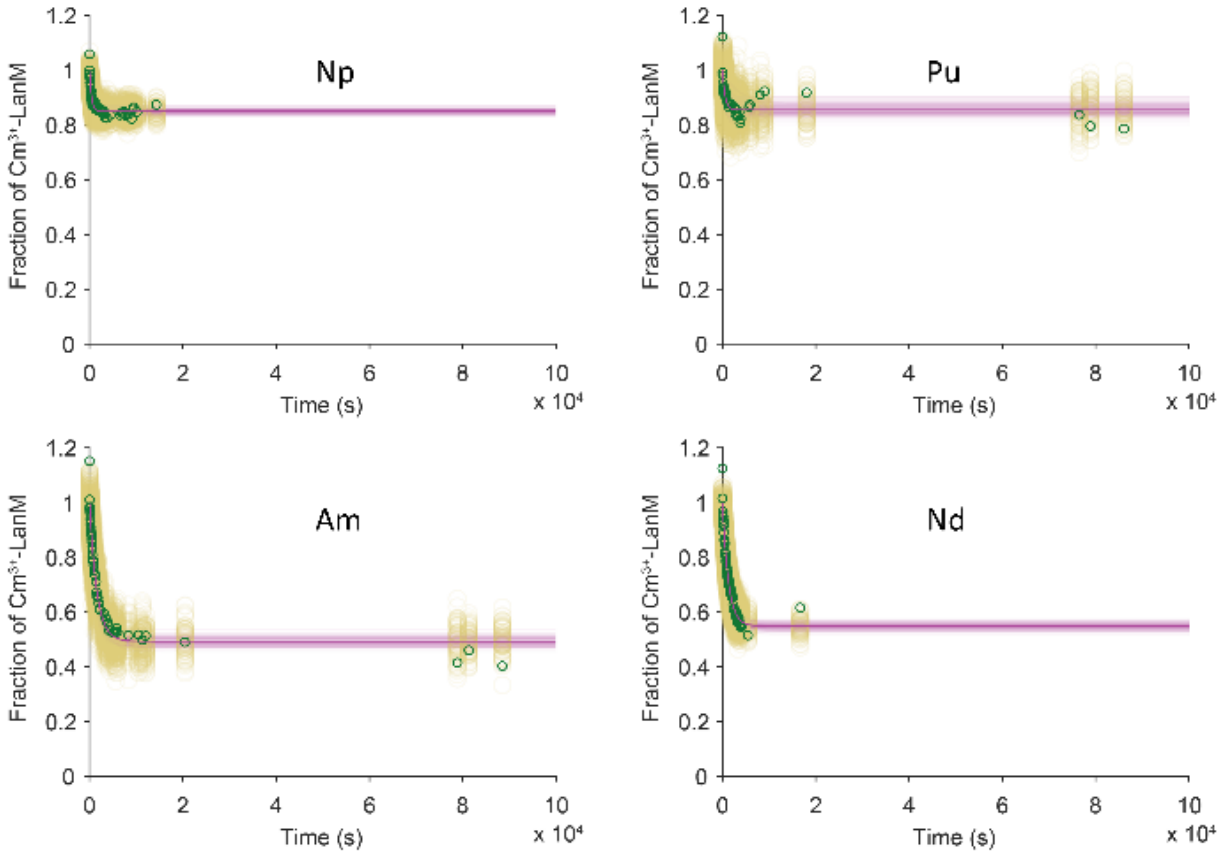

Figure S3. MC approach for the exchange experiments with Cm^{3+}. MC in yellow compared to raw data in green (fits in magenta).

3. Results and Discussion

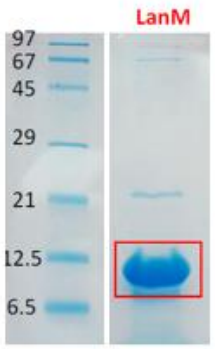

Figure S4. SDS-PAGE of the purified protein LanM.

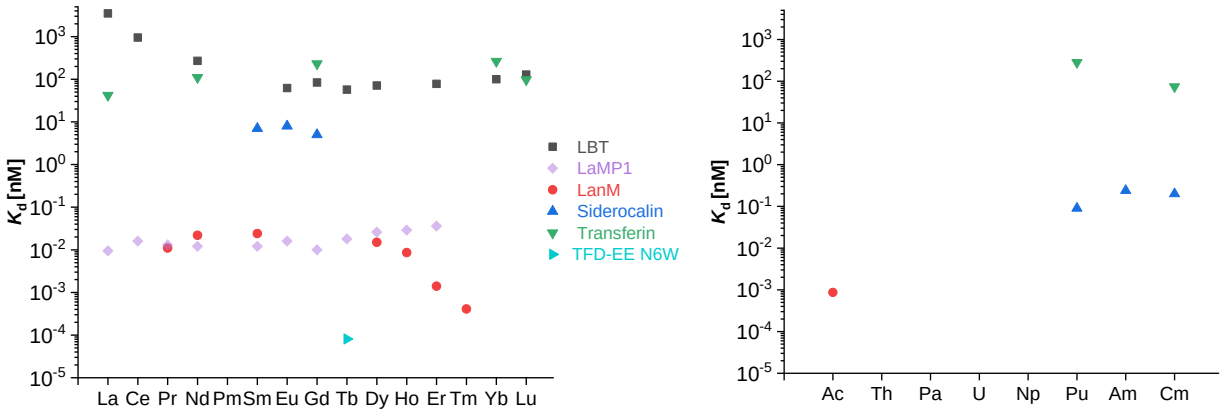

Figure S5. Previously reported affinity constants for Ln and An of Ln-binding systems LBT[4] and LaMP1[5] or proteins which were described to bind Lns LanM,[6, 7] TFD-EE N6W,[8, 9] Siderocalin,[10] Transferrin[11]. Measurements regarding the LBT were performed with fluorescence spectroscopy at pH 7.0 in 10 mM N-2-hydroxyethylpiperazine-N'-2-ethanesulfonic acid (HEPES) buffer and 100 mM NaCl. K_d of LaMP1 was obtained by FRET ratios with EDDS-buffered metal solutions at pH 7.2 in 30 mM MOPS and 100 mM KCl. For LanM, K_d was determined with UV-Vis spectrophotometry at pH 5 in 100 mM KCl/K-acetate buffer. Studies regarding Siderocalin were done with fluorescence quenching analysis at pH 7.4 in 100 mM HEPES buffer. Pu was provided for the experiments in oxidation state +IV. Binding constants of Transferrin were obtained with HPLC measurements in NH_4HCO_3 buffer at pH 7.4. TFD-EE N6W was studied with EGTA-buffered solutions in 25 mM HEPES and 100 mM NaCl at pH 7.5 in combination with sensitized luminescence.

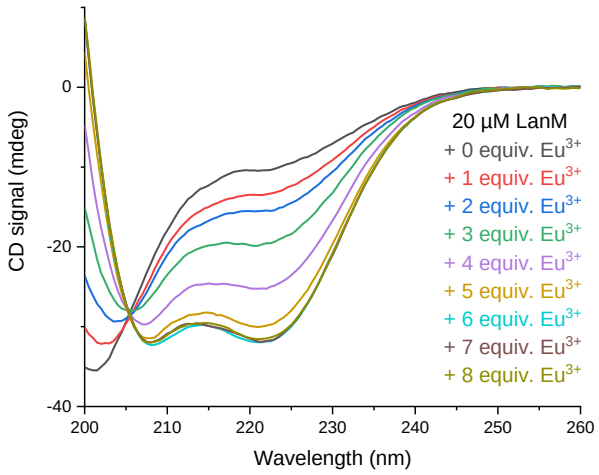

Figure S6. CD-spectra of 20 µM apo-LanM with addition of different equivalents of Eu^{3+}.

Table S1. Intensities of Eu^{3+}-LanM and Cm^{3+}-LanM signal of figure 4 and 6 and calculated time constants of figure 3C and 5C.

Element	Eu^{3+}-LanM signal (%)	Cm^{3+}-LanM signal (%)	Time constants (s)
La^{3+}	69.71	-	1222.00
Ce^{3+}	62.43	-	1094.30
Pr^{3+}	58.92	-	811.48
Nd^{3+}	49.73	51.77	986.60 (Eu) / 1334.80 (Cm)
Pm^{3+}	-	-	-
Sm^{3+}	60.38	-	767.52
Gd^{3+}	67.35	-	648.95
Tb^{3+}	68.31	-	692.92
Dy^{3+}	78.16	-	647.12
Ho^{3+}	76.49	-	483.83
Er^{3+}	80.93	-	482.49
Tm^{3+}	81.19	-	378.40
Yb^{3+}	82.14	-	453.53
Lu^{3+}	89.51	-	167.80
Np	-	76.50	426.15
Pu	-	69.02	416.87
Am^{3+}	-	42.10	1461.80

Table S2. Ionic radii of Ln and An and their oxidation states[12]

Element	Ionic radius (pm)[a]	Oxidation states[b]
La	103.2	+ III
Ce	101.0	**+ III**, +IV
Pr	99.0	**+ III**, +IV
Nd	98.3	+ III
Pm	97.0	+ III
Sm	95.8	+ II, **+ III**
Eu	94.7	+ II, **+ III**
Gd	93.8	+ III
Tb	92.3	**+ III**, +IV
Dy	91.2	+ III
Ho	90.1	+ III
Er	89.0	+ III
Tm	88.0	+ III
Yb	86.8	+ II, **+ III**
Lu	86.1	+ III
Np	101.1	+ III, + IV, **+V**, +VI, +VII
Pu	99.5	+ III, **+ IV**, +V, +VI, +VII
Am	98.0	**+ III**, + IV, +V, +VI
Cm	97.0	**+ III**, + IV

[a] Ionic radii for +III oxidation state [b] in bold the most prevalent one, not well characterized or solid-state oxidation states were not included

The redox chemistry of Ans differs completely from the Lns. While Am and Cm only reveal a few oxidation states, Np and Pu have multitudes which also coexist. Factors like pH or the presence of reducing or oxidizing reagents as well as complexing agents and the concentration of the element itself play an important role. For a better overview, relevant notes on the oxidations important for the discussion are given.

Table S3. Notes on the versatile redox chemistry of the actinides[12, 13]

Element	Oxidation state	Ionic radius (pm)[a]	Note
Np	III	101.1	Np^{3+}; stable in aqueous acidic solution but gets easily oxidized in the presence of air to $Np^{4+}$and NpO_2^+
Np	IV	87.4	Np^{4+}; stable in aqueous solution but slow oxidation to NpO_2^+ was observed with air, in low acidic environment also hydrolysis was described
Np	V	n.a..	Dioxo species NpO_2^+; most stable form in aqueous solution, disproportionation 2 NpO_2^+ + 4 H^+ ⇌ Np^{4+} + NpO_2^{2+} + 2 H_2O only described at high concentrations or at strongly acidic environment, formation of hydroxides in neutral and basic environment
Np	VI	n.a.	Dioxo species NpO_2^{2+}; mainly present at acidic pH but reduction to NpO_2^+ was described, formation of hydroxides in neutral and basic environment
Pu	III	99.5	Pu^{3+}; stable in aqueous acidic solution and on air but is easily oxidized to Pu^{4+}
Pu	IV	85.9	Pu^{4+}, only stable in highly acidic environment, with lower acidic conditions a disproportionation to $Pu^{3+}$and PuO_2^{2+} was described as well as the formation of colloidal hydrolysis products
Pu	V	n.a.	Dioxo species PuO_2^+, is unstable and disproportion to Pu^{4+} and PuO_2^{2+} was described, in aqueous solutions the formation of Pu^{3+} and PuO_2^{2+} was observed
Pu	VI	n.a.	Dioxo species PuO_2^{2+}, reduction to Pu^{4+} in acidic medium was described
Am	III	98.0	Stable and not easy to oxidize
Am	IV	84.8	Fluorides or carbonates in aqueous solution
Cm	III	97.0	Stable
Cm	IV	84.1	Fluorides CmF_4 in aqueous solution, CmO_2, ion stable in aqueous solutions with highly complexing agents

[a] n.a. = not available

Table S4. Published dissociation constants K_d for Ln and LanM[1, 6, 9]
Please note that the different K_d were determined with various methods which explains the strong deviations. Also, intrinsic and apparent K_d are listed here.

	Average intrinsic K_d[b]6	Apparent K_d [c]9	Apparent K_d [d]1
3 La^{3+} + LanM = La_3LanM	n.d.[a]	n.d.	5.3 ± 0.6 pM
3 Pr^{3+} + LanM = Pr_3LanM	11 ± 1 pM	70 ± 10 pM	n.d.
3 Nd^{3+} + LanM = Nd_3LanM	22 ± 2 pM	n.d.	5.3 ± 0.6 pM
3 Sm^{3+} + LanM = Sm_3LanM	24 ± 6 pM	n.d.	6.6 ± 2.8 pM
3 Gd^{3+} + LanM = Gd_3LanM	n.d.	100 ± 10 pM	10 ± 4 pM
3 Tb^{3+} + LanM = Tb_3LanM	n.d.	n.d.	21 ± 2 pM
3 Dy^{3+} + LanM = Dy_3LanM	15 ± 4 pM	200 ± 50 pM	n.d.
3 Ho^{3+} + LanM = Ho_3LanM	8.6 ± 1.4 pM	260 ± 60 pM	2.5 ± 0.4
3 Er^{3+} + LanM = Er_3LanM	1.4 ± 0.2 pM	n.d.	n.d.
3 Tm^{3+} + LanM = Tm_3LanM	0.41 ± 0.13 pM	n.d.	n.d.

[a] n.d. = not determined [b] determined with UV-Vis spectrophotometry at pH 5 in 100 mM KCl/K-acetate buffer [c] determined with CD spectroscopy in combination with chelator-buffered solutions at pH 5, buffer with 20 mM acetate and 100 mM KCl [d] determined with CD spectroscopy at pH 7.0 in buffer 20 mM MOPS, 20 mM acetate and 100 mM KCl

Supporting References

1. J. A. Cotruvo, E. R. Featherston, J. A. Mattocks, J. V. Ho and T. N. Laremore, *J. Am. Chem. Soc.*, 2018, **140**, 15056-15061.
2. C. Andersson and R. Bro, *Chemom. Intell. Lab. Syst.*, 2000, **52**, 1-4.
3. B. Drobot, M. Schmidt, Y. Mochizuki, T. Abe, K. Okuwaki, F. Brulfert, S. Falke, S. A. Samsonov, Y. Komeiji, C. Betzel, T. Stumpf, J. Raff and S. Tsushima, *Phys. Chem. Chem. Phys.*, 2019, **21**, 21213-21222.
4. M. Nitz, M. Sherawat, K. J. Franz, E. Peisach, K. N. Allen and B. Imperiali, *Angew. Chem. Int. Ed.*, 2004, **43**, 3682-3685.
5. J. A. Mattocks, J. V. Ho and J. A. Cotruvo, *J. Am. Chem. Soc.*, 2019, **141**, 2857-2861.
6. G. J. P. Deblonde, J. A. Mattocks, D. M. Park, D. W. Reed, J. A. Cotruvo and Y. Jiao, *Inorg. Chem.*, 2020, **59**, 11855-11867.
7. G. J. P. Deblonde, J. A. Mattocks, Z. Dong, P. T. Wooddy, J. A. J. Cotruvo, M. Zavarin, *ChemRxiv* 2021, DOI 10.26434/chemrxiv.14763426.v1. This content is a preprint and has not been peer-reviewed. Now available as Capturing an elusive but critical element: Natural protein enables actinium chemistry. *Sci. Adv.* 2021, **7**, eabk0273.
8. S. J. Caldwell, I. C. Haydon, N. Piperidou, P.-S. Huang, M. J. Bick, H. S. Sjöström, D. Hilvert, D. Baker and C. Zeymer, *Proc. Natl. Acad. Sci. U.S.A.*, 2020, **117**, 30362.
9. J. A. Mattocks, J. L. Tirsch and J. A. Cotruvo, in *Methods Enzymol.*, ed. J. A. Cotruvo, Academic Press, 2021, vol. 651, pp. 23-61.
10. B. E. Allred, P. B. Rupert, S. S. Gauny, D. D. An, C. Y. Ralston, M. Sturzbecher-Hoehne, R. K. Strong and R. J. Abergel, *Proc. Natl. Acad. Sci. U.S.A.*, 2015, **112**, 10342-10347.
11. G. J. P. Deblonde, M. Sturzbecher-Hoehne, A. B. Mason and R. J. Abergel, *Metallomics*, 2013, **5**, 619-626.
12. G. T. Seaborg and D. E. Hobart, *Summary of the properties of the lanthanide and actinide elements*, Indian Association of Nuclear Chemists and Allied Scientists, India, 1996.
13. L. R. Morss, N. M. Edelstein, J. Fuger, J. J. Katz and L. Morss, *The chemistry of the actinide and transactinide elements*, Springer, 2006.